



HAL
open science

Dynamic response of a circular tunnel with imperfect surface interaction embedded in an elastic medium

Rezgar Shakeri, Arnaud Mesgouez, Gaëlle Lefeuvre-Mesgouez

► To cite this version:

Rezgar Shakeri, Arnaud Mesgouez, Gaëlle Lefeuvre-Mesgouez. Dynamic response of a circular tunnel with imperfect surface interaction embedded in an elastic medium. CFM 2017 - 23ème Congrès Français de Mécanique, Aug 2017, Lille, France. hal-03465597

HAL Id: hal-03465597

<https://hal.science/hal-03465597v1>

Submitted on 3 Dec 2021

HAL is a multi-disciplinary open access archive for the deposit and dissemination of scientific research documents, whether they are published or not. The documents may come from teaching and research institutions in France or abroad, or from public or private research centers.

L'archive ouverte pluridisciplinaire **HAL**, est destinée au dépôt et à la diffusion de documents scientifiques de niveau recherche, publiés ou non, émanant des établissements d'enseignement et de recherche français ou étrangers, des laboratoires publics ou privés.

Dynamic response of a circular tunnel with imperfect surface interaction embedded in an elastic medium

R. SHAKERI^a, A. MESGOUEZ^b, G. LEFEUVE-MESGOUEZ^c

[a, b, c] Université d'Avignon et des Pays de Vaucluse (UAPV) UMR 1114 EMMAH, Campus Jean-Henri Fabre, Agroparc, 301 rue Baruch de Spinoza, BP 21239, 84916 Avignon cedex 9 - France.
rezgarshakeri@gmail.com

Résumé

Le travail proposé ici fait partie d'un projet plus global traitant de la caractérisation du sous-sol par des approches ondulatoires dans le cadre unique du Laboratoire Souterrain à Bas Bruit (LSBB) de Rustrel, Vaucluse, France. L'environnement expérimental actuel du LSBB fait apparaître un ensemble de galeries horizontales souterraines (plusieurs centaines de mètres sous terre), dont une galerie principale qui présente une paroi bétonnée. Une galerie dite anti-souffle est, quant à elle, restée brute après percement. La première étape de notre travail consiste à mettre en place un problème direct permettant d'appréhender cette géométrie spécifique. Nous proposons ainsi d'établir dans ce papier, par une approche semi-analytique, la réponse bidimensionnelle en régime transitoire de la galerie principale, présentant une partie bétonnée en surface, elle-même baignée dans un espace rocheux infini, homogène, isotrope et élastique de toute part. Les conditions de contact entre la paroi et la roche sont considérées comme imparfaites, faisant apparaître une discontinuité de déplacement à l'interface tunnel-sol. Une excitation de type point source à l'intérieur du tunnel est prise en compte. Dans un premier temps, le problème est résolu dans le domaine fréquentiel. Les champs mécaniques dans le tunnel et le sol sont exprimés en utilisant des séries de Hankel ou Bessel adaptées. La prise en compte des conditions aux limites spécifiques conduit à la résolution, pour chaque mode et pour chaque fréquence, d'un système linéaire permettant de déterminer les termes des séries nécessaires à l'estimation numérique des champs de contraintes et de déplacements en tout point de la géométrie. L'algorithme de Durbin est alors utilisé pour revenir dans l'espace temporel à partir de l'ensemble des réponses fréquentielles. Les deux approches, harmonique et temporelle, sont validées sur des cas limites issus de la bibliographie. Pour finir, l'étude de l'influence de différents paramètres est proposée : épaisseur de la partie bétonnée du tunnel, qualité des interfaces et enfin nature de la source excitatrice.

Abstract

The research work proposed here is part of a global project that aims at better characterizing a specific underground environment in the LSBB (Low Noise Inter-disciplinary Underground Science and Technology), situated in Rustrel, Vaucluse, France. The experimental environment under study is characterized by a system of galleries, several ones with a concrete layer. The first step of the methodology deals with setting up a forward problem to apprehend the geometry of the LSBB.

In this paper, the 2D transient response of imperfect bonded circular lined pipeline lying in an elastic, homogeneous and infinite medium is studied. At first, the problem is solved in the frequency domain by using the wave function expansion method and imperfect interaction surface between elastic medium and tunnel is modeled as a linear spring. Wave propagation fields in tunnel and soil are expressed in terms of infinite series and stresses and displacements are given based on those series. By implying boundary conditions a linear equations system is obtained and the results of these equations lead to displacement and stress responses of the rock and tunnel. To solve the transient problem, the Laplace transform with respect to time is used which leads to system of linear equations in the Laplace domain. Durbin's numerical Laplace transform inversion method is employed to obtain dynamic responses. To exhibit a behavior of the responses, influences of the different parameters such as wall thickness of the tunnel is investigated. Hoop stresses and the displacements of the tunnel and rock are obtained due to acting load on the inner surface of the tunnel for selected parameters. In order to check the validity of the present work, we pay attention on the convergence of the results and also excellent agreement with previous result is achieved.

Mots clefs : Dynamic response ; wave propagation ; imperfect interface ; circular tunnel ; analytical approach

Introduction

Underground structure analysis is a significant area of nonstop research in various fields such as civil engineering, mining and geophysics. Studying mechanical wave propagation in complex heterogeneous media, such as ground structures, is of great importance, not only for mechanical applications or seismic events, but also for medium because wave propagation signals contain information on the medium constitution. This latter point involves the study and construction of both forward and inverse problems. Many researchers considered the dynamic response of a cavity in an elastic medium or a pipeline subjected to dynamic load in rock medium with perfect boundary conditions. The present literature review focuses on harmonic and transient responses.

In harmonic or frequency domain, Singh et al [1] compared the analytical results of thick and thin shell theories which employed for orthotropic cylindrical shell formulation buried in an elastic linear, homogeneous and isotropic infinite medium. They concluded that the changing from thick to thin shell theory has significant effect on radial displacements for soft and hard soil conditions. Upadhyay and Mishra [2, 3] studied non-axisymmetric 2D dynamic response of orthotropic thick cylindrical shell embedded in a linear elastic, homogeneous and isotropic medium subjected by a combination of P, SV and SH harmonic waves analytically. They found that the shell deformation of flexural mode may be even greater than in the axisymmetric mode in soft and hard soil conditions and wave speed. Dwivedi and Upadhyay [4] considered an imperfect bonded thick infinite orthotropic pipeline subjected to harmonic P-wave in order to study the effects of the imperfect interaction surface between soil and shell on the displacement under condition of soft and stiff soil. Rao et al [5] studied a buried infinite orthotropic cylindrical shell, subjected by P-wave in the surrounding ground. The shell is assumed to be thin, perfectly bonded to the infinite elastic medium. Harmonic axial and hoop stresses only for axisymmetric mode of the shell for different soil conditions and orthotropy parameters has been investigated. They found that the stresses in the pipes can be minimized by choosing the best orthotropy parameters. Thambiratnam and Lee [6]

presented a simple approximately method for the scattering of plane harmonic SH-waves by arbitrary shape's cavity in full or half space homogeneous, elastic medium by discretizing the interface of the cavity with soil into a series of straight strips. They concluded that the incidence's angle influences the displacement greatly and changing the strip size does not lead to significant variation in results. Lee and Karl [7] studied the scattering and diffraction of plane harmonic SV waves by cylindrical cavity in an elastic half space analytically. They found the significant influences of different parameters such as the incidence's angle, the cavity depth, the dimensionless frequency of the incident wave and Poisson's ratio on the surface displacement. De Barros and Luco [8] obtained the 2D response of an infinitely long, cylindrical cavity excited by harmonic plane waves and surfaces waves in layered viscoelastic, homogeneous half-space by applying an indirect boundary integral method based on moving Green's functions. They used the same approach to achieve harmonic response of the long cylindrical shell under the same conditions of the soil and waves [9, 10]. Stamos and Beskos [11] investigated 2D cylindrical tunnel of a concrete buried in an elastic, homogeneous materials subjected to seismic waves and obtained the responses by using the direct boundary element method. Manoogian [12] applied the weighted residual method to study the scattering and diffraction of harmonic SH waves by an arbitrary shape's tunnel which is embedded in 2D elastic half space. He considered the effects of different shapes of tunnel, angle of incidence and wave's frequency on ground surface amplitudes. Davis et al [13] investigated the response of underground cavity to harmonic SV waves in an elastic half space by using analytical method. They extended analytical solutions to approximate solutions for determining hoop stresses in cavity liner. They compared dynamic response of buried pipe which obtained by approximate solutions with existing results of 1994 Northridge earthquake. Karakostas and Manolis [14] evaluated the harmonic response of different cavities in an elastic medium with randomness in its properties by using a stochastic boundary element method. They considered different numerical examples like circular, elliptical and two circular cavities to demonstrate the adaptability of SBEM formulation. Kouretzis et al [15] employed 3D shell theory to obtain strain and hoop stress of cylindrical tunnel subjected to harmonic shear waves. The soil medium was considered as an elastic, homogeneous half-space or soft soil overlays the bedrock. They studied the bedrock effects and uniform ground condition in order to calculate axial, hoop and the von Mises strains by using analytical and numerical methods. Esmaili et al [16] investigated harmonic response of circular tunnel in an elastic full space subjected by P-SV waves. They used hybrid boundary, and finite element methods to calculate the hoop stresses in the lining and interface of tunnel and soil. El Naggari et al [17] presented jointed cylindrical tunnel embedded in linear elastic soil under seismic-induced shear waves. They modeled the outer tunnel as a thick-walled cylinder which can be used as a degraded zone around the tunnel approximately, and the inner tunnel as a thin-walled shell. By using the analytical solution, the effects of jointed tunnel, thickness of degraded zone and incidence angle on the stresses of lining are investigated for slip and no slip conditions. Yu and Dravinski [18] studied scattering of harmonic P, SV or Rayleigh waves by a 2D corrugated cavity embedded in an isotropic, elastic half-space and full-space by using a direct boundary integral equation method. The differences between the rough and smooth cavity lead to significant changes in the displacement results. They concluded that neglecting the roughness of the scatterer may result in errors in the responses. Lin et al [19] presented an analytical formulation of the boundary-valued problem to apply zero-stress boundary conditions at the half space easily. They considered 2D cylindrical tunnel in a half-space elastic medium with harmonic incident plane P-waves and the influences of different parameters on the response were studied. Coskun et al [20] analyzed the 2D dynamic responses of circular cavity in an elastic half-space subjected to a uniformly distributed harmonic pressure at the inner surface of the cavity by using analytical solution

and the effects of the wave number and cavity depth on the displacements and stresses are presented. Liu et al [21] used an analytical approach to solve the scattering of harmonic plane P, SV or Rayleigh waves by cylindrical tunnel in an elastic half space. They introduced Mobius transformation to map the medium onto concentric circles and by applying the boundary conditions, a set of infinite algebraic equations are formulated. Their results indicate that the embedment's depth, the shear modulus and the thickness of the liner have major effects on the dynamic responses of the lining and elastic medium. Gomes et al [22] studied the effect of ground stratification on the seismic response of circular tunnel embedded in an elastic, homogeneous medium by using FEM methods. They proved that ground stratification has an important role in the lining seismic forces. Kara [23] calculated analytically the diffraction of harmonic plane SH waves by cylindrical tunnel embedded in homogeneous, isotropic and elastic quarter-space. He satisfied boundary conditions at inner and outer tunnel surface directly and stress-free boundary conditions on the surface ground satisfied via imaging method and addition theorems. Lin et al [24] presented a procedure for seismic analysis for circular tunnel based on 2.5D finite/infinite element approach. They found that stress concentrations on the inner surface are larger than those in outer surface and also for earthquake consideration the stresses caused by SV-waves are much larger than those by P-waves. In reality, the interface between tunnel and rock is imperfect due to micro-cracks in the interface and wall roughness. A few papers modeled imperfect interface as a linear spring [25, 26] or a parallel linear dashpot and spring [27] and are solved analytically in the frequency domain. Yi et al [25, 26] investigated the dynamic response of circular tunnel with imperfect bonded interface in full space elastic medium subjected to plane and cylindrical P-waves. They modeled the imperfect boundary conditions as a spring and by using the analytical solution the influences of imperfect interface on the dynamic stress concentration factors (DSCF) in the lining and the rock are studied. Fang and Jin [27] proposed a visco-elastic interface model to study dynamic stress around a non-circular tunnel in an elastic medium subjected by harmonic P and SV waves. The visco-elastic imperfect boundary was modeled as linear spring and dashpot, and by using conformal mapping the non-circular tunnel transformed into annular region. They found that the effect of viscosity on dynamic stress in low frequency range is larger than high frequency range.

In the case of transient wave propagation or time response, Manolis et al [28] combined FEM and BEM methods to gain 3D responses of buried pipeline in soil. In fact they used the BEM methods for analysis the pipeline cavity in elastic soil which excited by unit displacement impulses on the free ground surface and using the results of BEM analysis as input for FEM solution of thin shell vibration. Tadeu et al [29] used the BEM method to study the 2D steady-state and transient wave scattering of arbitrary cavities shapes in an homogeneous, elastic medium which excited by dynamic sources in a half-space and full-space. Zakout and Akkas[30] used Residual Variable Method to obtain the transient response of long cylindrical cavity with and without thin elastic shell embedded in an elastic, isotropic medium. The displacements and stresses were presented under uniform Heaviside loading which acted on the inner surface. Karakostas and Manolis [31] used the BEM method and a simple perturbation-based probabilistic model for modeling the complex composition of the geological material to study the 2D cylindrical cavity in soil under different types of transient environmental load. They solved the transient problem in Laplace domain and an efficient inverse transformation method was employed to obtain time responses for series of numerical examples like cylindrical tunnels embedded in a stochastic geological medium under different type of excitations. Tadeu et al [32] obtained the 3D scattering field by an irregular, cylindrical cavity with infinite length embedded in homogeneous elastic medium excited by point load by using BEM method to study the influences of cross-sectional geometry of the cavity on the

waves propagating in frequency and time domain. Clouteau et al [33] solved 3D problem of tunnel-soil interaction using FEM method for tunnel and BEM formulation for the soil. The point load is applied on the invert of tunnel and the soil is assumed to be homogeneous and elastic. The displacement of the tunnel and free surface of the soil is obtained in frequency and time domain. Kouretzis et al [34] considered the strain in buried pipelines due to surface blast load. They modeled the pipeline as a 3D cylindrical thin shell and the surface blast load as a time-dependent vertical point load acting on the surface of a homogeneous, isotropic and elastic half space. They used the analytical results of strain analysis of P and Rayleigh waves and a good comparison with experimental results and simple design procedure are achieved. Feldgun et al [35] simulated the 3D and transient response of an explosion occurring inside a buried pipeline. The tunnel and soil are modeled as a Timoshenko elastic plastic shell, Grigoryan model that takes into account both bulk and shear elastic plastic behavior. The gas-dynamics problem inside the tunnel is solved by the modified Gudunov method. Smerzini et al [36] considered a theoretical approach to study the effects on underground structures (e.g. circular cavity, elastic shell) on surface motion embedded in 2D homogeneous, isotropic and linear visco-elastic halfspace subjected to seismic excitation in frequency and time domain. Tsaur and Chang [37] solved the 2D multiple scattering problem of horizontally-truncated circular cavity in an elastic medium excited by SH waves. They employed region-matching technique in cooperation with imaging's method and Graf's addition formula to obtain frequency and time responses of ground and cavity surfaces displacement. Panji et al [38] analyzed the 2D scalar wave problems in a isotropic elastic medium based on the half-plane time domain BEM method. They presented the different examples such as elastic half space without cavity and full/truncated circular cavity in an elastic medium to show some advantages of half-plane BEM method over the full-plane BEM. Kouretzis et al [39] presented a closed-form solution to calculate tunnel forces due to P-waves propagation in an elastic medium. Under the real assumption, they showed P-waves lead to higher axial hoop forces than S-waves and by using finite element code ABAQUS/Standard verified their results. Ptilakis et al [40] investigated the effect of above ground structures on tunnel responses in urban areas during the seismic excitation. Above ground structures are modeled as equivalent single-degree of freedom oscillators. They proved that the above ground structures effect are an increase of the tunnel dynamic response, lining bending moment and lining axial force especially for shallower burial depths. Chao-jiao et al [41] studied the transient response of cylindrical cavity buried in an elastic soil subjected to anti-plane impact load along the cavity axis direction. They solved the equations in Laplace transform and obtained time domain results by using analytical expressions of Laplace inverse transform and numerical Laplace inverse method (Durbin's method). Alielahi et al [42] used time-domain boundary element method to investigate a buried tunnel subjected to vertically propagating incident SV and P waves. They depicted the results for different shapes of tunnels, tunnel wall thickness, burial depths and truncated and discussed about their effects on dynamic ground surface and tunnel responses. Fu et al [43] studied soil-tunnel interaction of a rigid tunnel buried in elastic soil overlaying on elastic bedrock to P and SV waves excitations. They used indirect boundary element method with Green's function of distributed loads acting on inclined lines. They concluded that the dynamic displacement in layered half-space is larger than homogeneous one.

The above review clearly indicates that, while there exists a lot of literature on transient and harmonic wave propagation in an elastic medium, transient response of 2D tunnel with imperfect interface embedded in an elastic, homogeneous, and isotropic soil seems to be absent. In this study, the entire methodology is defined in the Laplace transform domain. Waves propagation fields in tunnel and soil are expressed in form of infinite series and stresses and displacements are given based on those series.

By implying imperfect boundary conditions a linear equations system is obtained and the results of these equations lead to displacement and stress responses of the rock and tunnel in Laplace domain. By using Durbin's inversion algorithm [44] the time responses of tunnel and soil are calculated semi-analytically.

Formulation

The problem configuration is illustrated in Fig. 1. A long cylindrical tunnel is embedded in an infinite soil medium. The outer radius of the tunnel is b and its inner radius is a .

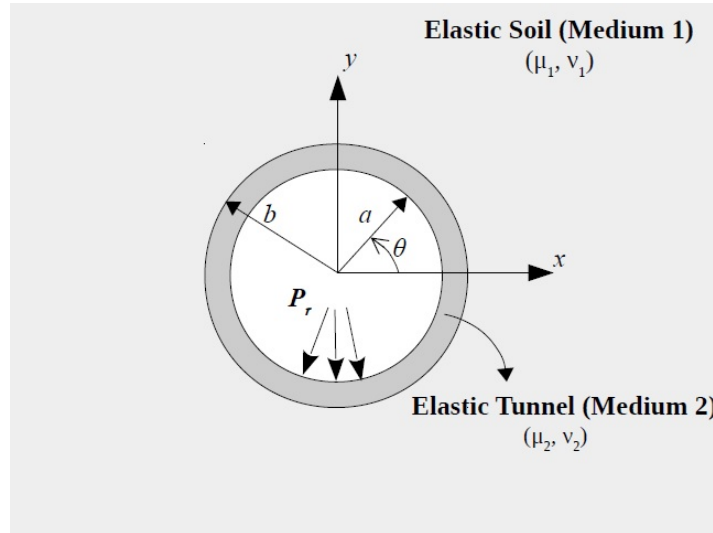


FIGURE 1 – Problem geometry

A transient internal load acts on the inner surface of tunnel tunnel as shown in Fig. 1. The displacement equations of motion for a homogeneous, isotropic and a linearly elastic medium can be written as [45]

$$\mu \nabla^2 \mathbf{u} + (\lambda + \mu) \nabla \nabla \cdot \mathbf{u} = \rho \ddot{\mathbf{u}}, \quad (1)$$

where μ , λ are Lamé constants, ρ is the material density, and the vector displacement \mathbf{u} can be decomposed into the gradient of a scalar potential ϕ and a vector potential Ψ as

$$\mathbf{u} = \nabla \phi + \nabla \times \Psi, \quad (2)$$

where the scalar and vector potentials satisfy the following wave equations

$$\nabla^2 \phi = \frac{1}{c_p^2} \ddot{\phi}, \quad (3)$$

$$\nabla^2 \Psi = \frac{1}{c_s^2} \ddot{\Psi}, \quad (4)$$

where $c_p = \sqrt{\frac{\lambda+2\mu}{\rho}}$ and $c_s = \sqrt{\frac{\mu}{\rho}}$ are the P-wave and SV-wave velocities in the elastic medium, respectively. The displacement field \mathbf{u} does not depend on the z -coordinate due to the 2D configuration, so the vector potential Ψ only has one single component ψ_z , and for simplicity it will be written as ψ . Applying the Laplace transform with respect to time ($\bar{f}(r, \theta, s) = \int_0^\infty f(r, \theta, t) e^{-st} dt$), to Eq.(3) and

Eq.(4), yield to

$$\frac{\partial^2 \bar{\phi}}{\partial r^2} + \frac{1}{r} \frac{\partial \bar{\phi}}{\partial r} + \frac{1}{r^2} \frac{\partial^2 \bar{\phi}}{\partial \theta^2} + \bar{\alpha}^2 \bar{\phi} = 0, \quad (5)$$

$$\frac{\partial^2 \bar{\psi}}{\partial r^2} + \frac{1}{r} \frac{\partial \bar{\psi}}{\partial r} + \frac{1}{r^2} \frac{\partial^2 \bar{\psi}}{\partial \theta^2} + \bar{\beta}^2 \bar{\psi} = 0, \quad (6)$$

where over-bar hereafter denotes the Laplace transform, $\bar{\alpha} = \frac{is}{c_p}$ and $\bar{\beta} = \frac{is}{c_s}$ are the wave numbers of P and SV-waves in the Laplace domain, respectively and $i = \sqrt{-1}$. The solutions of wave Eqs. (5) and (6) can be written as a combination of Hankel function and sine or cosine functions which will be presented later.

Waves in soil and tunnel

Due to the interface between the soil and the tunnel, two reflected waves (P and SV) in the soil medium will propagate when the load acts on inner surface of the tunnel. They are expressed by Hankel functions of the first kind that represent outgoing cylindrical waves. The total displacement potentials in the soil are [46]

$$\bar{\phi}_1^t = \sum_{n=0}^{\infty} A_n(s) H_n^1(\bar{\alpha}_1 r) \cos n\theta, \quad (7)$$

$$\bar{\psi}_1^t = \sum_{n=0}^{\infty} B_n(s) H_n^1(\bar{\beta}_1 r) \sin n\theta, \quad (8)$$

where $A_n(s)$ and $B_n(s)$ are unknown coefficients, H_n^1 is the Hankel function of the first kind of order n , $\bar{\beta}_1$ is the wave number of SV-wave in the soil, and the subscript 1 in $\bar{\phi}_1^t$ and $\bar{\psi}_1^t$ denotes the waves in the soil medium.

Tunnel medium which is in contact with soil at the outer circular surface $r = b$ has two incoming cylindrical waves (P and SV) and two outgoing cylindrical waves. The two incoming P and SV- waves which propagate to the inside of the lining from the outer circular surface at $r = b$ can be presented by Hankel functions of the second kind. The two outgoing P and SV-waves that propagate from the inner surface at $r = a$ can be written by Hankel functions of the first kind. Generally, the total displacement potentials in the tunnel are [46]

$$\bar{\phi}_2^t = \sum_{n=0}^{\infty} [C_n(s) H_n^2(\bar{\alpha}_2 r) + D_n(s) H_n^1(\bar{\alpha}_2 r)] \cos n\theta, \quad (9)$$

$$\bar{\psi}_2^t = \sum_{n=0}^{\infty} [M_n(s) H_n^2(\bar{\beta}_2 r) + N_n(s) H_n^1(\bar{\beta}_2 r)] \sin n\theta, \quad (10)$$

where $C_n(s)$, $D_n(s)$, $M_n(s)$ and $N_n(s)$ are unknown coefficients, H_n^2 is the Hankel function of the second kind of order n , $\bar{\alpha}_2$ and $\bar{\beta}_2$ are wave numbers of P and SV waves in the lining, and subscript 2 in $\bar{\phi}_2^t$ and $\bar{\psi}_2^t$ denotes the waves in the tunnel.

Displacement and Stress Expansion

Based on the relations between the displacement vector and the scalar and vector potentials, Eq. (2), and stress-strain relations, as represented by Hooke's law, the displacement and stress components in an

elastic medium in polar coordinates and the Laplace domain can be written as

$$\bar{u}_r = \frac{\partial \bar{\phi}}{\partial r} + \frac{1}{r} \frac{\partial \bar{\psi}}{\partial \theta}, \quad (11)$$

$$\bar{u}_\theta = \frac{1}{r} \frac{\partial \bar{\phi}}{\partial \theta} - \frac{\partial \bar{\psi}}{\partial r}, \quad (12)$$

$$\bar{\sigma}_{rr} = \lambda \nabla^2 \bar{\phi} + 2\mu \left[\frac{\partial^2 \bar{\phi}}{\partial r^2} + \frac{\partial}{\partial r} \left(\frac{1}{r} \frac{\partial \bar{\psi}}{\partial \theta} \right) \right], \quad (13)$$

$$\bar{\sigma}_{\theta\theta} = \lambda \nabla^2 \bar{\phi} + 2\mu \left[\frac{1}{r} \left(\frac{\partial \bar{\phi}}{\partial r} + \frac{1}{r} \frac{\partial^2 \bar{\phi}}{\partial \theta^2} \right) + \frac{1}{r} \left(\frac{1}{r} \frac{\partial \bar{\psi}}{\partial \theta} - \frac{\partial^2 \bar{\psi}}{\partial r \partial \theta} \right) \right], \quad (14)$$

$$\bar{\sigma}_{r\theta} = \mu \left[\frac{2}{r} \left(\frac{\partial^2 \bar{\phi}}{\partial r \partial \theta} - \frac{1}{r} \frac{\partial \bar{\phi}}{\partial \theta} \right) + \left(\frac{1}{r^2} \frac{\partial^2 \bar{\psi}}{\partial \theta^2} - r \frac{\partial}{\partial r} \left(\frac{1}{r} \frac{\partial \bar{\psi}}{\partial r} \right) \right) \right], \quad (15)$$

By substituting the potential functions, Eqs. (7) and (8) into the above equations, displacements and stresses of the soil medium in the Laplace domain are obtained as follow

$$\bar{u}_{r1} = r^{-1} \sum_{n=0}^{\infty} [A_n(s) e_{11}(\bar{\alpha}_1 r) + B_n(s) e_{12}(\bar{\beta}_1 r)] \cos n\theta, \quad (16)$$

$$\bar{u}_{\theta 1} = r^{-1} \sum_{n=0}^{\infty} [A_n(s) e_{21}(\bar{\alpha}_1 r) + B_n(s) e_{22}(\bar{\beta}_1 r)] \sin n\theta, \quad (17)$$

$$\bar{\sigma}_{rr1} = 2\mu_1 r^{-2} \sum_{n=0}^{\infty} [A_n(s) e_{31}(\bar{\alpha}_1 r) + B_n(s) e_{32}(\bar{\beta}_1 r)] \cos n\theta, \quad (18)$$

$$\bar{\sigma}_{\theta\theta 1} = 2\mu_1 r^{-2} \sum_{n=0}^{\infty} [A_n(s) e_{41}(\bar{\alpha}_1 r) + B_n(s) e_{42}(\bar{\beta}_1 r)] \cos n\theta, \quad (19)$$

$$\bar{\sigma}_{r\theta 1} = 2\mu_1 r^{-2} \sum_{n=0}^{\infty} [A_n(s) e_{51}(\bar{\alpha}_1 r) + B_n(s) e_{52}(\bar{\beta}_1 r)] \sin n\theta, \quad (20)$$

and substitution of Eqs. (9) and (10) into Eqs. (11)-(15), give the displacements and stresses in the Laplace domain for tunnel as

$$\begin{aligned} \bar{u}_{r2} = r^{-1} \sum_{n=0}^{\infty} & \left[C_n(s) e_{13}(\bar{\alpha}_2 r) + D_n(s) e_{11}(\bar{\alpha}_2 r) \right. \\ & \left. + M_n(s) e_{14}(\bar{\beta}_2 r) + N_n(s) e_{12}(\bar{\beta}_2 r) \right] \cos n\theta, \end{aligned} \quad (21)$$

$$\begin{aligned} \bar{u}_{\theta 2} = r^{-1} \sum_{n=0}^{\infty} & [C_n(s) e_{23}(\bar{\alpha}_2 r) + D_n(s) e_{21}(\bar{\alpha}_2 r) \\ & + M_n(s) e_{24}(\bar{\beta}_2 r) + N_n(s) e_{22}(\bar{\beta}_2 r)] \sin n\theta, \end{aligned} \quad (22)$$

$$\begin{aligned} \bar{\sigma}_{rr2} = 2\mu_2 r^{-2} \sum_{n=0}^{\infty} [C_n(s)e_{33}(\bar{\alpha}_2 r) + D_n(s)e_{31}(\bar{\alpha}_2 r) \\ + M_n(s)e_{34}(\bar{\beta}_2 r) + N_n(s)e_{32}(\bar{\beta}_2 r)] \cos n\theta, \end{aligned} \quad (23)$$

$$\begin{aligned} \bar{\sigma}_{\theta\theta2} = 2\mu_2 r^{-2} \sum_{n=0}^{\infty} [C_n(s)e_{43}(\bar{\alpha}_2 r) + D_n(s)e_{41}(\bar{\alpha}_2 r) \\ + M_n(s)e_{44}(\bar{\beta}_2 r) + N_n(s)e_{42}(\bar{\beta}_2 r)] \cos n\theta, \end{aligned} \quad (24)$$

$$\begin{aligned} \bar{\sigma}_{r\theta2} = 2\mu_2 r^{-2} \sum_{n=0}^{\infty} [C_n(s)e_{53}(\bar{\alpha}_2 r) + D_n(s)e_{51}(\bar{\alpha}_2 r) \\ + M_n(s)e_{54}(\bar{\beta}_2 r) + N_n(s)e_{52}(\bar{\beta}_2 r)] \sin n\theta, \end{aligned} \quad (25)$$

where μ_1 and μ_2 are the respective Lamé constants for the soil and lining, the e_{ij} are defined in Appendix A and the unknown coefficients $A_n(s) \dots N_n(s)$ can be obtain by applying the boundary conditions.

Imperfect boundary conditions

We assume here the imperfect boundary conditions at the interface of the rock and the tunnel. In fact, rock mass has various discontinuities like foliation, faults and joints and these discontinuities have significant effects on the dynamic response of tunnel. One of the famous models for modeling the imperfect boundary conditions is the linear spring model. In this model, displacements are assumed discontinuous along the entire length of the interface but tractions are continuous. Based on this concept, the imperfect boundary conditions at the interface surface between the lining and soil at $r = b$ are [26, 45]

$$\bar{\sigma}_{rr1} = \bar{\sigma}_{rr2}, \quad (26)$$

$$\bar{\sigma}_{r\theta1} = \bar{\sigma}_{r\theta2}, \quad (27)$$

$$\bar{\sigma}_{rr1} = k_r(\bar{u}_{r1} - \bar{u}_{r2}), \quad (28)$$

$$\bar{\sigma}_{r\theta1} = k_\theta(\bar{u}_{\theta1} - \bar{u}_{\theta2}), \quad (29)$$

and the boundary conditions at the inner surface of the lining at $r = a$

$$\bar{\sigma}_{rr2} = P_r, \quad (30)$$

$$\bar{\sigma}_{r\theta2} = 0, \quad (31)$$

where k_r and k_θ are normal and tangential spring constants respectively and P_r is the internal load. Two different types of internal load are considered. First, a step distributed load with amplitude P_0 , acts on the whole inner surface of the tunnel at $r = a$ which can be expressed in Laplace domain as $P_r = P_0/s$. Second, an impulse point load acts on the inner surface at point $(r, \theta) = (a, 0)$; in the Laplace domain is $P_r = \frac{\delta(\theta)}{a} P_0$, where $\delta(\theta)$ is Dirac delta function. The term $\frac{\delta(\theta)}{a}$ can be expanded into the Fourier cosine

series [47]

$$\frac{\delta(\theta)}{a} = \sum_{n=0}^{\infty} \frac{\epsilon_n}{\pi a} \cos(n\theta), \quad (32)$$

where $\epsilon_n = 1/2$ for $n = 0$ and $\epsilon_n = 1$ for $n \geq 1$. Also, the step load can be expanded into the Fourier cosine series as follow

$$\frac{P_0}{s} = \sum_{n=0}^{\infty} \epsilon_n \cos(n\theta), \quad (33)$$

where $\epsilon_n = P_0/s$ for $n = 0$ and $\epsilon_n = 0$ for $n \geq 1$. In fact, physically the step load acts on the tunnel uniformly which only excites the symmetric modes, and Hankel or Bessel functions of zero order are symmetric.

By truncating the linear systems of Eqs. (26)-(31), with N being the truncation constant, these linear equations can be put in the matrix form

$$\mathbf{E}(s)\mathbf{Q}(s) = \mathbf{F}(s), \quad (34)$$

where

$$\mathbf{Q}(s) = [A_n(s), B_n(s), C_n(s), D_n(s), M_n(s), N_n(s)]^T, \quad (35)$$

$$\mathbf{F}(s) = [0, 0, 0, 0, p_{rn}, 0]^T, \quad (36)$$

and

$$\mathbf{E}(s) = \begin{bmatrix} -\bar{\mu}e_{31}(\bar{\alpha}_1 b) & -\bar{\mu}e_{32}(\bar{\alpha}_1 b) & e_{33}(\bar{\alpha}_2 b) & e_{31}(\bar{\alpha}_2 b) & e_{34}(\bar{\alpha}_2 b) & e_{32}(\bar{\alpha}_2 b) \\ -\bar{\mu}e_{51}(\bar{\alpha}_1 b) & -\bar{\mu}e_{52}(\bar{\alpha}_1 b) & e_{53}(\bar{\alpha}_2 b) & e_{51}(\bar{\alpha}_2 b) & e_{54}(\bar{\alpha}_2 b) & e_{52}(\bar{\alpha}_2 b) \\ \frac{2\mu_1}{bk_r}e_{31}(\bar{\alpha}_1 b) - e_{11}(\bar{\alpha}_1 b) & \frac{2\mu_1}{bk_r}e_{32}(\bar{\alpha}_1 b) - e_{12}(\bar{\alpha}_1 b) & e_{13}(\bar{\alpha}_2 b) & e_{11}(\bar{\alpha}_2 b) & e_{14}(\bar{\alpha}_2 b) & e_{12}(\bar{\alpha}_2 b) \\ \frac{2\mu_1}{bk_\theta}e_{51}(\bar{\alpha}_1 b) - e_{21}(\bar{\alpha}_1 b) & \frac{2\mu_1}{bk_\theta}e_{52}(\bar{\alpha}_1 b) - e_{22}(\bar{\alpha}_1 b) & e_{23}(\bar{\alpha}_2 b) & e_{21}(\bar{\alpha}_2 b) & e_{24}(\bar{\alpha}_2 b) & e_{22}(\bar{\alpha}_2 b) \\ 0 & 0 & e_{33}(\bar{\alpha}_2 a) & e_{31}(\bar{\alpha}_2 a) & e_{34}(\bar{\alpha}_2 a) & e_{32}(\bar{\alpha}_2 a) \\ 0 & 0 & e_{43}(\bar{\alpha}_2 a) & e_{41}(\bar{\alpha}_2 a) & e_{44}(\bar{\alpha}_2 a) & e_{42}(\bar{\alpha}_2 a) \end{bmatrix} \quad (37)$$

where $\bar{\mu} = \frac{\mu_1}{\mu_2}$, $p_{rn} = P_0 a^2 / 2s\mu_2$ for $n=0$, $p_{rn} = 0$ for $n \geq 1$ in the case of a step load, and $p_{rn} = P_0 / 2a\pi$ for $n = 0$ and $p_{rn} = P_0 / a\pi$ for $n \geq 1$ in the case of an impulse point load. Solving Eq. (34) for different values of n gives the $A_n(s) \dots N_n(s)$ in the Laplace domain. Next, the inversion of Laplace transforms are performed numerically by using the following Durbin's formula in the interval $[0, 2T_0]$ [44]

$$\Lambda(t) = \frac{2e^{ct}}{T_0} \left[\frac{1}{2} \text{Re}[\bar{\Lambda}(c)] + \sum_{k=1}^M \left[\text{Re}[\bar{\Lambda}(c + \frac{2\pi ik}{T_0})] \cos(\frac{2\pi kt}{T_0}) - \text{Im}[\bar{\Lambda}(c + \frac{2\pi ik}{T_0})] \sin(\frac{2\pi kt}{T_0}) \right] \right], \quad (38)$$

where M is the truncation parameter, c is an arbitrary real number and $\bar{\Lambda}(s)$ can be any of $\bar{u}_r(s)$, $\bar{u}_\theta(s)$, $\bar{\sigma}_{rr}(s)$, and $\bar{\sigma}_{\theta\theta}(s)$. The suggested value of cT_0 and M are between 5-10, and 50-5000 for sufficient accuracy [44], respectively.

Numerical Results

Validation

Before presenting the main results, our formulation is validated by comparison with results found in the literature. Due to the lack of transient response with imperfect boundary condition, first, the harmonic response of a tunnel embedded in an elastic soil subjected to plane P wave is obtained. Fig. 2 exhibits the dynamic stress concentration factor $\sigma_{\theta\theta}^*$ of the lining at $r = a$ which is defined as [26]

$$\sigma_{\theta\theta}^* = \left| \frac{\sigma_{\theta\theta}}{\sigma_0} \right|, \quad (39)$$

where $\sigma_0 = \mu_1 \beta_1^2 \phi_0$. The soil and lining parameters in Fig. 2 are $\nu_1 = 0.25$, $\nu_2 = 0.2$, $\frac{\mu_1}{\mu_2} = 2.9$, $\frac{C_{p1}}{C_{p2}} = 1.5$, $\frac{b}{a} = 1.2$ and $\alpha_1 a = 0.1$. Excellent agreement between present results and [26] for different values of k_r and k_θ is achieved.

Second, in order to show the reliability of transient response, a cylindrical cavity in the elastic medium

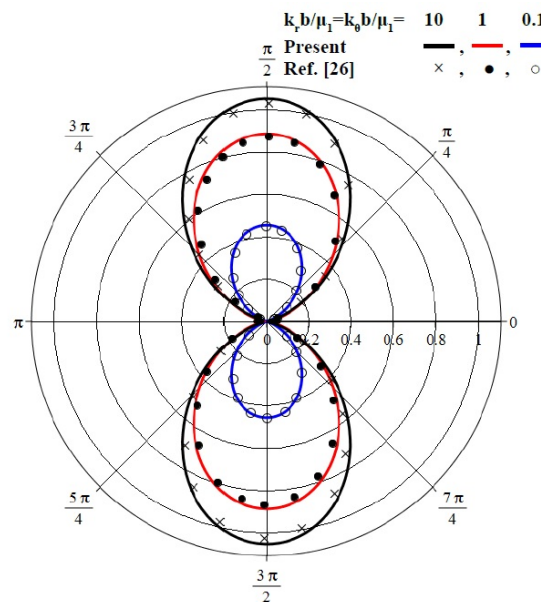


FIGURE 2 – Hoop stress comparison of the present results and [26] for different values of k_r and k_θ

under a step load which acted on the inner surface of the cavity is considered [30]. Our geometry is equivalent to [30] by choosing the following parameters $\nu_1 = \nu_2 = 0.3$, $C_{p1} = C_{p2} = \sqrt{3.5}$, $\mu_1 = \mu_2 = 1$, $a = 1$, $b = 1.2$, $C_{s1} = C_{s2} = 1$ and $k_r = k_\theta = \frac{100\mu_1}{b}$. A big value for spring in the interface between the soil and lining changes the imperfect boundary condition to a perfect interface. Also, the same materials for lining and soil are considered to get a one elastic medium. In this case the present result and [30] are compared and good agreement, as shown in Fig.3, is achieved for $n = 0$.

Main Results

The main results are obtained by choosing the material properties as $\nu_1 = 0.25$, $\nu_2 = 0.3$, $\mu_1/\mu_2 = 0.31$, $C_{p1}/C_{p2} = 0.7$, and in Durbin's formula $M = 500$, $c = 5$ and $T_0 = 60$. Fig. 4 displays the dimensionless displacements of the rock u_{r1}/a at $r = b$ and u_{r2}/a at $r = a = 1$ for different thicknesses of the tunnel's wall and spring stiffnesses of imperfect boundary condition and for a step load. For small

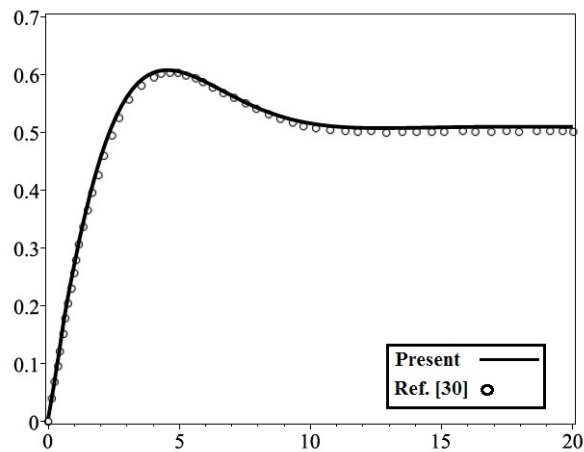


FIGURE 3 – Comparison of the nondimensional displacement respect to the nondimensional time for $n = 0$

values of k_r and k_θ , due to flexible contact between the rock and the tunnel, displacements are very large and fluctuation is clear. When the values of stiffness increase, the interface acts as a perfectly bonded. In fact, flexibility of the boundary condition decreases and there is no fluctuation for big values of k_r and k_θ .

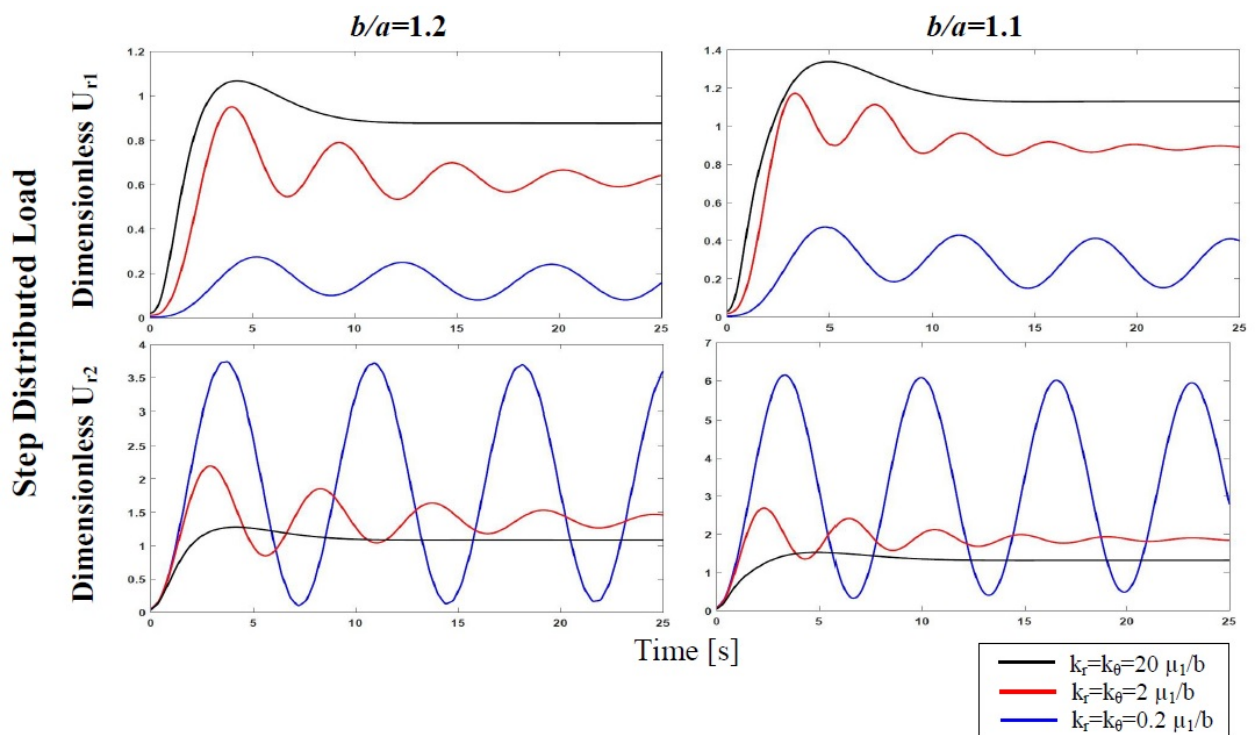


FIGURE 4 – Dimensionless displacement of rock (u_{r1}/a) at $r = b$ and tunnel (u_{r2}/a) at $r = a = 1m$ for different ratio of b/a , k_r and k_θ

Fig. 5 shows the dimensionless hoop stresses for the rock $\sigma_{\theta\theta 1}/\mu_2$ at $r = b$ and tunnel $\sigma_{\theta\theta 2}/\mu_2$ at $r = a$ ($\mu_2 = 1$). It is clear that for small values of stiffness the fluctuation can be observed due to flexibility of the interface between rock and tunnel. When the stiffness increases the hoop stress decreases and less oscillations occur.

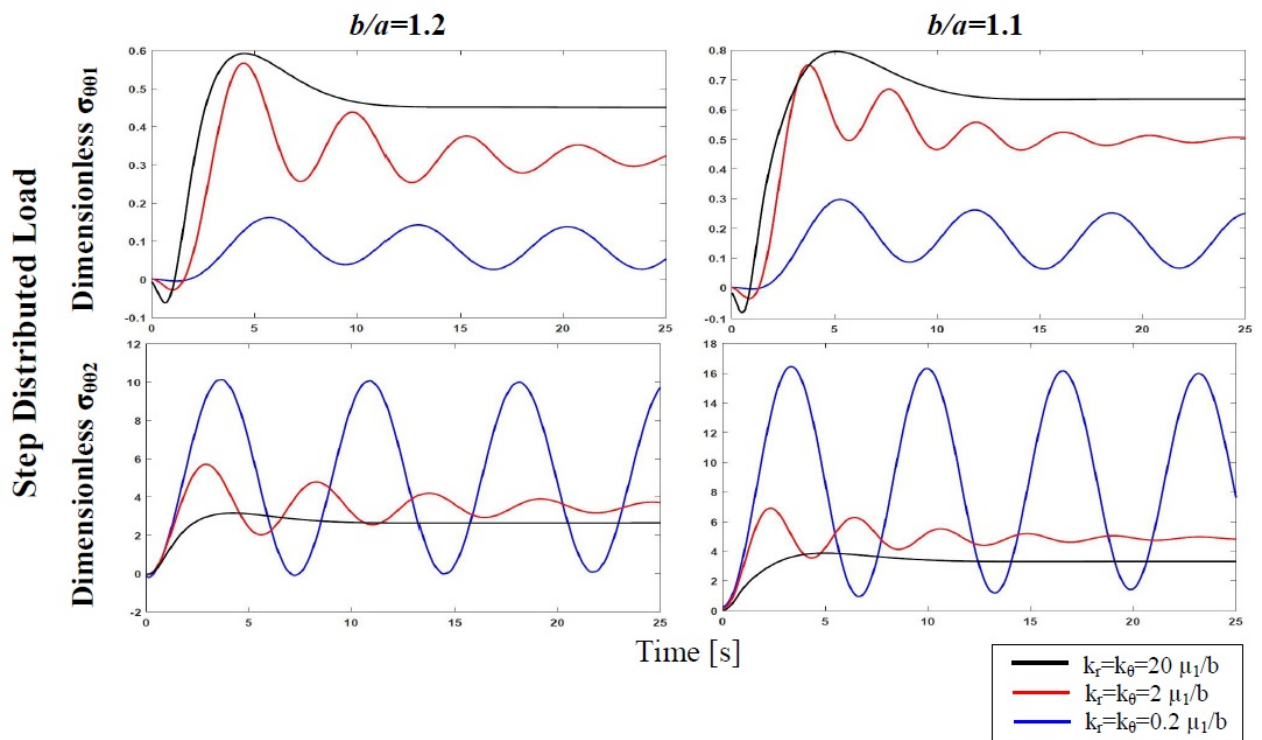


FIGURE 5 – Dimensionless hoop stresses of rock ($\sigma_{\theta\theta 1}/\mu_2$) at $r = b$ and tunnel ($\sigma_{\theta\theta 2}/\mu_2$), ($\mu_2 = 1Pa$) at $r = a = 1m$ for different ratio of b/a , k_r and k_θ

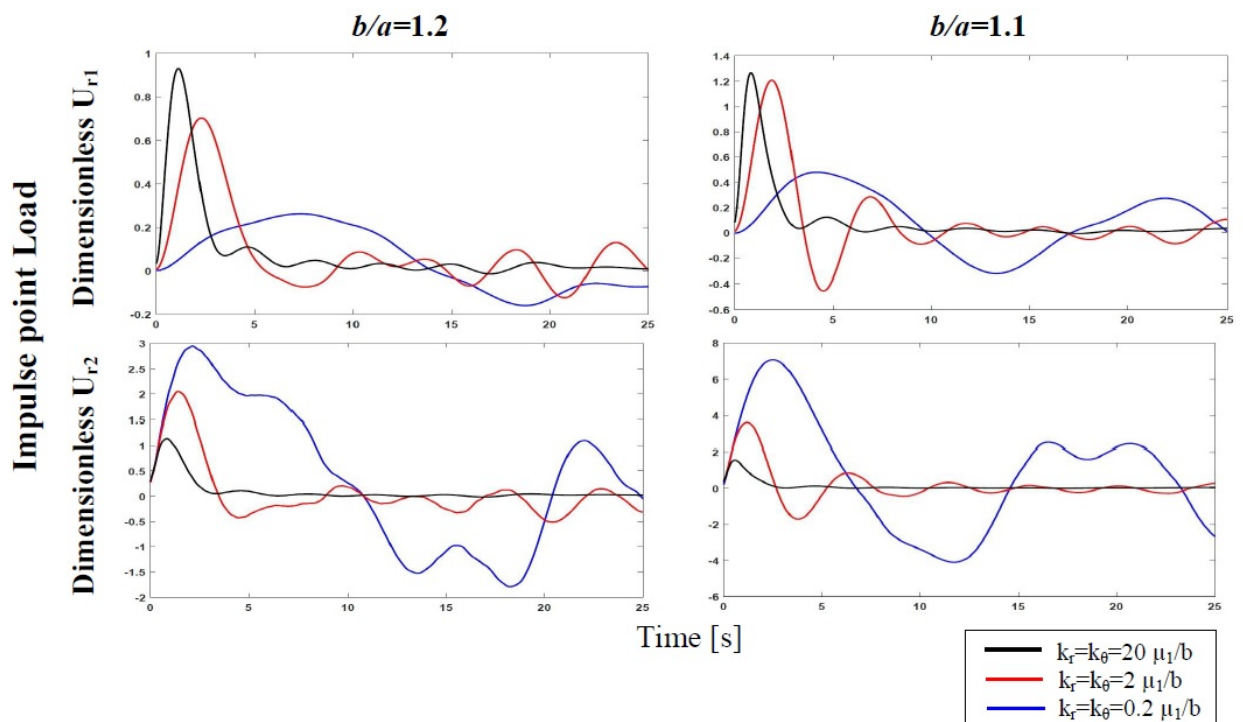


FIGURE 6 – Dimensionless displacement of rock (u_{r1}/a) at $r = b$ and tunnel (u_{r2}/a) at $r = a = 1m$ for different ratio of b/a , k_r and k_θ

Figs. 6 and 7 show the dimensionless displacement and hoop stresses of the rock and the tunnel for an impulse point load. The displacements and stresses of the rock and the tunnel behave like the step

load case for different values of thickness and stiffness. In contrast, because the impulsive load acts on the tunnel for very short period, the displacement or stress oscillate around original static equilibrium position, regardless of thickness ratio. But in the case of the step load, due to a constant load which applies on the system continually, the oscillation is around a different equilibrium position.

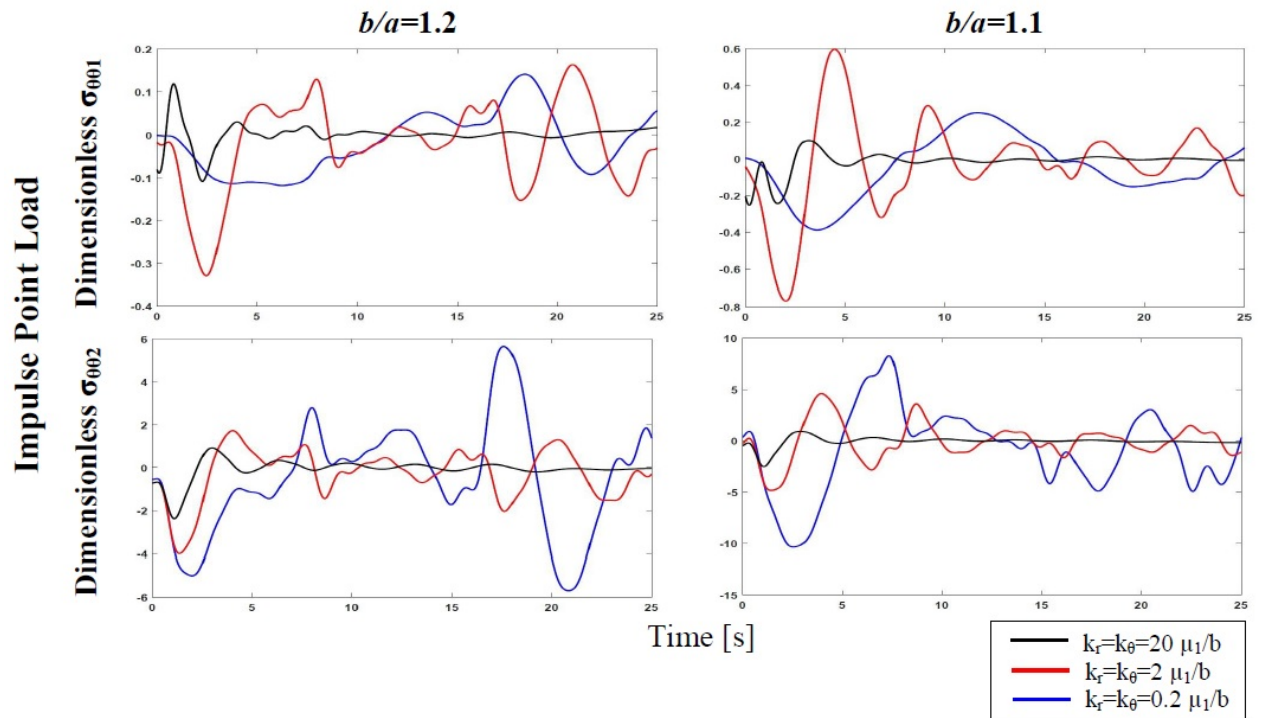


FIGURE 7 – Dimensionless hoop stresses of rock ($\sigma_{\theta\theta 1}/\mu_2$) at $r = b$ and tunnel ($\sigma_{\theta\theta 2}/\mu_2$) ($\mu_2 = 1Pa$) at $r = a = 1m$ for different ratio of b/a , k_r and k_θ

Conclusion

In this paper, the 2D dynamic responses of the tunnel subjected to the internal transient load with imperfect boundary conditions is studied analytically. The interface of the rock and tunnel is assumed to be imperfect and is modeled as a normal and transverse linear spring. By applying the Laplace transform, the wave equations are presented in the Laplace domain. Based on the Hooke's law and employing the potentials functions, displacements and stresses for rock and tunnel medium are expanded in series form. Satisfying the imperfect boundary conditions leads to system of equations and the unknown coefficients are obtained in the Laplace domain. Using the Durbin's formula the results in time domain are acquired and the most important observations are summarized as follows :

- In the case of weak bonded in an interface, the displacements and hoop stresses of the tunnel are large due to flexible bonded.
- Increasing the value of spring coefficients leads to decreasing of displacements and hoop stresses.
- When the impulse point load is applied to the tunnel, the system vibrate around original equilibrium position because the impulse load acts on the system suddenly and once the forcing function is removed, the tunnel and rock start oscillating freely.
- In contrast, in step load case the fluctuation is around different equilibrium position due to acting of step load permanently.

Appendix

$$\begin{aligned}
e_{11}(\bar{\alpha}r) &= \bar{\alpha}r H_{n-1}^1(\bar{\alpha}r) - n H_n^1(\bar{\alpha}r), \\
e_{12}(\bar{\beta}r) &= n H_n^1(\bar{\beta}r), \\
e_{13}(\bar{\alpha}r) &= \bar{\alpha}r H_{n-1}^2(\bar{\alpha}r) - n H_n^2(\bar{\alpha}r), \\
e_{14}(\bar{\beta}r) &= n H_n^2(\bar{\beta}r), \\
e_{21}(\bar{\alpha}r) &= -n H_n^1(\bar{\alpha}r), \\
e_{22}(\bar{\beta}r) &= -\bar{\beta}r H_{n-1}^1(\bar{\beta}r) + n H_n^1(\bar{\beta}r), \\
e_{23}(\bar{\alpha}r) &= -n H_n^2(\bar{\alpha}r), \\
e_{24}(\bar{\beta}r) &= -\bar{\beta}r H_{n-1}^2(\bar{\beta}r) + n H_n^2(\bar{\beta}r), \\
e_{31}(\bar{\alpha}r) &= (n^2 + n - \frac{1}{2}\bar{\beta}^2 r^2) H_n^1(\bar{\alpha}r) - \bar{\alpha}r H_{n-1}^1(\bar{\alpha}r), \\
e_{32}(\bar{\beta}r) &= n[-(n+1) H_n^1(\bar{\beta}r) + \bar{\beta}r H_{n-1}^1(\bar{\beta}r)], \\
e_{31}(\bar{\alpha}r) &= (n^2 + n - \frac{1}{2}\bar{\beta}^2 r^2) H_n^2(\bar{\alpha}r) - \bar{\alpha}r H_{n-1}^2(\bar{\alpha}r), \\
e_{32}(\bar{\beta}r) &= n[-(n+1) H_n^2(\bar{\beta}r) + \bar{\beta}r H_{n-1}^2(\bar{\beta}r)], \\
e_{41}(\bar{\alpha}r) &= -(n^2 + n + \frac{1}{2}\bar{\beta}^2 r^2 - \bar{\alpha}^2 r^2) H_n^1(\bar{\alpha}r) + \bar{\alpha}r H_{n-1}^1(\bar{\alpha}r), \\
e_{42}(\bar{\beta}r) &= n[(n+1) H_n^1(\bar{\beta}r) - \bar{\beta}r H_{n-1}^1(\bar{\beta}r)], \\
e_{43}(\bar{\alpha}r) &= -(n^2 + n + \frac{1}{2}\bar{\beta}^2 r^2 - \bar{\alpha}^2 r^2) H_n^2(\bar{\alpha}r) + \bar{\alpha}r H_{n-1}^2(\bar{\alpha}r), \\
e_{44}(\bar{\beta}r) &= n[(n+1) H_n^2(\bar{\beta}r) - \bar{\beta}r H_{n-1}^2(\bar{\beta}r)], \\
e_{51}(\bar{\alpha}r) &= -n[-(n+1) H_n^1(\bar{\alpha}r) + \bar{\alpha}r H_{n-1}^1(\bar{\alpha}r)], \\
e_{52}(\bar{\alpha}r) &= -(n^2 + n - \frac{1}{2}\bar{\beta}^2 r^2) H_n^1(\bar{\beta}r) + \bar{\beta}r H_{n-1}^1(\bar{\beta}r), \\
e_{53}(\bar{\alpha}r) &= -n[-(n+1) H_n^2(\bar{\alpha}r) + \bar{\alpha}r H_{n-1}^2(\bar{\alpha}r)], \\
e_{54}(\bar{\alpha}r) &= -(n^2 + n - \frac{1}{2}\bar{\beta}^2 r^2) H_n^2(\bar{\beta}r) + \bar{\beta}r H_{n-1}^2(\bar{\beta}r)
\end{aligned}$$

Références

- [1] V.P. Singh, P.C. Upadhyay, B. Kishor, A comparison of thick and thin shell theory results for buried orthotropic cylindrical shells, *Journal of Sound and Vibration*, 119 (1987) 339–345.
- [2] P.C. Upadhyay, B.K. Mishra, Non-axisymmetric dynamic response of a buried orthotropic cylindrical shell due to incident shear waves, *Journal of Sound and Vibration*, 125 (1988) 227–239.
- [3] P.C. Upadhyay, B.K. Mishra, Non-axisymmetric dynamic response of buried orthotropic cylindrical shells, *Journal of Sound and Vibration*, 121 (1988) 149–160.
- [4] J.P. Dwivedi, P.C. Upadhyay, Effect of imperfect bonding on the axisymmetric dynamic response of buried orthotropic cylindrical shells, *Journal of Sound and Vibration*, 135 (1989) 477–486.
- [5] P.V.M. Rao, V.P. Singh, P.C. Upadhyay, Axisymmetric stresses in buried thin orthotropic cylindrical shells due to P-wave loading, *Composite Structures*, 13 (1989) 209–216.

- [6] D.P. Thambiratnam, S.L. Lee, Scattering of plane SH-waves by underground cavities, *Engineering Structures*, 12 (1990) 215–221.
- [7] V.W Lee, J Karl, Diffraction of SV waves by underground, circular, cylindrical cavities, *Soil Dynamics and Earthquake Engineering*, 11 (1992) 445–456.
- [8] F.C.P. de Barros, J.E. Luco, Diffraction of obliquely incident waves by a cylindrical cavity embedded in a layered viscoelastic half-space, *Soil Dynamics and Earthquake Engineering*, 12 (1993) 159–171.
- [9] J.E. Luco, F.C.P. de Barros, Seismic response of a cylindrical shell embedded in a layered viscoelastic half-space. I : Formulation, *Earthquake Engineering and Structural Dynamics*, 23 (1994) 553–567.
- [10] F.C.P. de Barros, J.E. Luco, Seismic response of a cylindrical shell embedded in a layered viscoelastic half-space. II : Validation and numerical results, *Earthquake Engineering and Structural Dynamics*, 23 (1994) 569–580.
- [11] A.A. Stamos, D.E. Beskos, 3-D seismic response analysis of long lined tunnels in half-space, *Soil Dynamics and Earthquake Engineering*, 15 (1996) 111–118.
- [12] M.E. Manoogian, Scattering and diffraction of SH waves above an arbitrarily shaped tunnel, *ISET Journal of Earthquake Technology*, 37 (2000) 11–26.
- [13] C.A. Davis, V.W. Lee, J.P. Bardet, Transverse response of underground cavities and pipes to incident SV waves, *Earthquake Engineering and Structural Dynamics*, 30 (2001) 383–410.
- [14] Ch.Z. Karakostasa, G.D. Manolis, Dynamic response of tunnels in stochastic soils by the boundary element method, *Engineering Analysis with Boundary Elements*, 26 (2002) 667–680.
- [15] G. P. Kouretzisa, G. D. Bouckovalasa, Ch. J. Gantesb, 3-D shell analysis of cylindrical underground structures under seismic shear (S) wave action, *Soil Dynamics and Earthquake Engineering*, 26 (2006) 909–921.
- [16] M. Esmaili, S. Vahdani, A. Noorzad, Dynamic response of lined circular tunnel to plane harmonic waves, *Tunnelling and Underground Space Technology*, 21 (2006) 511–519.
- [17] H.El.Naggar, S.D.Hinchberger, M.El.Naggar, Simplified analysis of seismic in-plane stresses in composite and jointed tunnel linings, *Soil Dynamics and Earthquake Engineering*, 28 (2008) 1063–1077.
- [18] Ch.W. Yu, M. Dravinski, Scattering of plane harmonic P, SV or Rayleigh waves by a completely embedded corrugated cavity, *Geophysical Journal International*, 178 (2009) 479–487.
- [19] Ch.H. Lin, V.W.Lee, M.I.Todorovska, M.D.Trifunac, Zero-stress, cylindrical wave functions around a circular underground tunnel in a flat, elastic half-space : Incident P-waves, *Soil Dynamics and Earthquake Engineering*, 30 (2010) 879–894.
- [20] I. Coskun, H. Engin, A. Ozmutlu, Dynamic Stress and Displacement in an Elastic Half-Space with a Cylindrical Cavity, *Shock and Vibration*, 18 (2011) 827–838.
- [21] Q.Liu, M. Zhao, L. Wang, Scattering of plane P, SV or Rayleigh waves by a shallow lined tunnel in an elastic half space, *Soil Dynamics and Earthquake Engineering*, 49 (2013) 52–63.
- [22] R.C. Gomes, F. Gouveia, D. Torcato, J. Santos, Seismic response of shallow circular tunnels in two-layered ground, *Soil Dynamics and Earthquake Engineering*, 75 (2015) 37–43.
- [23] H.F. Kara, A note on response of tunnels to incident SH-waves near hillsides, *Soil Dynamics and Earthquake Engineering*, 90 (2016) 138–146.

- [24] K.C. Lin, H.H.Hung, J.P.Yang, Y.B.Yang, Seismic analysis of underground tunnels by the 2.5D finite/infinite element approach, *Soil Dynamics and Earthquake Engineering*, 85 (2016) 31–43.
- [25] C.P. Yi, P. Zhang, D. Johansson, U. Nyberg, Dynamic response of a circular lined tunnel with an imperfect interface subjected to cylindrical P-waves, *Computers and Geotechnics*, 55 (2014) 165–171.
- [26] C.P. Yi, W.b. Lu, P. Zhang, D. Johansson, U. Nyberg, Effect of imperfect interface on the dynamic response of a circular lined tunnel impacted by plane P-waves, *Tunnelling and Underground Space Technology*, 21 (2016) 68–74.
- [27] X.Qi. Fang, H.X. Jin, Visco-elastic imperfect bonding effect on dynamic response of a non-circular lined tunnel subjected to P and SV waves, *Soil Dynamics and Earthquake Engineering*, 88 (2016) 1–7.
- [28] G.D. Manolis, P.I. Tetepoulidis, D.G. Talaslidis, G. Apostolidis, Seismic analysis of buried pipeline in a 3D soil continuum, *Engineering Analysis with Boundary Elements*, 15 (1995) 371–394.
- [29] A.J.B. Tadeu, Scattering of waves by subterranean structures via the boundary element method, *Soil Dynamics and Earthquake Engineering*, 15 (1996) 387–397.
- [30] U. Zakout, N. Akkas, Transient response of a cylindrical cavity with and without a bonded shell in an infinite elastic medium, *International Journal of Engineering Science*, 35 (1997) 1203–1220.
- [31] Ch. Z. Karakostas, G. D. Manolis, Dynamic response of unlined tunnels in soil with random properties, *Engineering Structures*, 22 (2000) 1013–1027.
- [32] A.J.B. Tadeu, J.M.P. Antonioa, E. Kausel, 3D scattering of waves by a cylindrical irregular cavity of infinite length in a homogeneous elastic medium, *Computer Methods in Applied Mechanics and Engineering*, 191 (2002) 3015–3033.
- [33] D. Clouteau, M. Arnst, T.M. Al-Hussainia, G. Degrande, Freefield vibrations due to dynamic loading on a tunnel embedded in a stratified medium, *Journal of Sound and Vibration*, 283 (2005) 173–199.
- [34] G.P. Kouretzis, G.D. Bouckovalas, Ch.J. Gantes, Analytical calculation of blast-induced strains to buried pipelines, *International Journal of Impact Engineering*, 34 (2007) 1683–1704.
- [35] V.R. Feldgun, A.V. Kochetkov, Y.S. Karinski, D.Z. Yankelevsky, Internal blast loading in a buried lined tunnel, *International Journal of Impact Engineering*, 35 (2008) 172–183.
- [36] C. Smerzini, J. Aviles, R. Paolucci, F. J. Sanchez-Sesma, Effect of underground cavities on surface earthquake ground motion under SH wave propagation, *Earthquake Engineering and Structural Dynamics*, 38 (2009) 1441–1460.
- [37] D.H. Tsaur, K.H. Chang, Multiple Scattering of SH Waves by an Embedded Truncated Circular Cavity, *Journal of Marine Science and Technology*, 20 (2012) 73–81.
- [38] M. Panji, M. Kamalian, J. Asgari Marnani, M. K. Jafari, Transient analysis of wave propagation problems by half-plane BEM, *Geophysical Journal International*, 194 (2013) 1849–1865.
- [39] G.P. Kouretzis, K.I. Andrianopoulos, S.W. Sloan, J.P. Carter, Analysis of circular tunnels due to seismic P-wave propagation, with emphasis on unreinforced concrete liners, *Computers and Geotechnics*, 55 (2014) 187–194.
- [40] K. Pitilakis, G. Tsinidis, A. Leanza, M. Maugeri, Seismic behaviour of circular tunnels accounting for above ground structures interaction effects, *Computers and Geotechnics*, 67 (2014) 1–15.

- [41] Z. Chao-jiao, X. Tang-dai, D. Guo-qing, D. Zhi, Dynamic response of cylindrical cavity to antiplane impact load by using analytical approach, *Journal of Central South University*, 21 (2014) 405–415.
- [42] H. Alielahi, M. Kamalian, M. Adampira, Seismic ground amplification by unlined tunnels subjected to vertically propagating SV and P waves using BEM, *Soil Dynamics and Earthquake Engineering*, 71 (2015) 63–79.
- [43] J. Fu, J. Liang, L. Qin, Dynamic soil-tunnel interaction in layered half-space for incident P and SV waves, *Earthquake Science*, 28 (2015) 275–284.
- [44] F. Durbin, Numerical inversion of Laplace transforms : an effective improvement of Dubner and Abate's method, *Comput Journal*, 8 (1973) 371–376.
- [45] J.D. Achenbach, *Wave propagation in elastic solids*, North-Holland, 2005.
- [46] Y.H. Pao, C.C. Mow *Diffraction of elastic waves and dynamics stress concentration*, New York : Crane Russak, 1973.
- [47] Z. Yuan, Y. Cai, Zh. Cao, An analytical model for vibration prediction of a tunnel embedded in a saturated full-space to a harmonic point load, *Soil Dynamics and Earthquake Engineering*, 86 (2016) 25–40.